P-ISSN : 2598-1277
E-ISSN : 2621-3966

JOURNAL OF GREEN SCIENCE AND TECHNOLOGY

SEISMIC PERFORMANCE EVALUATION USING PUSHOVER ANALYSIS OF FOUR TWO-STOREY RESIDENTIAL BUILDING TYPES IN WEST BANDUNG REGENCY

Joesack Renaldi Sugianto[1], Yosafat Aji Pranata[1*]

[1]) Master of Civil Engineering Program, Universitas Kristen Maranatha, Bandung.
[*]E-mail:yosafat.ap@maranatha.ac.id

ABSTRACT

In seismic-actively located West Bandung Regency it is crucial for evaluation of existing residential buildings seismic performance to mitigate potential earthquake losses. The purpose of this study was to study four standard two-storey reinforced concrete residential houses type A–D in West Bandung Regency using nonlinear static pushover analysis in SAP2000 and two main directions (X and Y). Performance points were established using the FEMA 440 equivalent linearization approach by crossing the capacity spectrum with the seismic demand spectrum, including stiffness degradation and effective damping due to nonlinear response. The seismic performance was analyzed in terms of some of the most common response indicators (spectral acceleration, spectral displacement, effective period or ductility, effective damping) and an empirical FEMA 356 plastic hinge assessment to establish the dominant mechanism of the damage. This shows a high directional dependency between spectral demand and displacement capacity among building types. The distribution of hinge states at the performance point is characterized by early–to-moderate damage types (A–B, B–IO, and IO–LS), with more severe states (LS–CP, CP–C, and isolated C–D) present in certain situations and localized. In conclusion the nonlinearity of the response is best characterized by a beam dominant mechanism indicating ductile behavior, however localized advanced hinge states indicate the requirement for targeted strengthening at critical members and directions.

Keyword: *pushover analysis; FEMA 440; performance point; plastic hinge; residential buildings.*

1. INTRODUCTION

West Bandung Regency, West Java, has been exposed to strong seismic activity as well as tectonic processes. The updated Indonesian Seismicity Map 2024 shows that West Java continues to be a high seismically vulnerable area [1]. This situation makes earthquake resistant design, and importantly seismic performance evaluation of existing buildings, remain a priority, particularly in the case of residential buildings that make up a high proportion of the building stock and are often constructed without detailed seismic verification [2].

A majority of the currently constructed two-story dwellings in Indonesia are made of RC frames with masonry infill walls. Although infill walls are often assumed as passive components, their contact with RC frames is likely to significantly influence initial stiffness, lateral strength, and the mode of failure. Neglecting the contribution of infill may result in false predictions of lateral capacity, drift demand, and damage distribution under seismic load [3], [4]. For practically based analytical modeling to handle this phenomenon, a macro model using an equivalent diagonal strut is often used for its simplicity and good accuracy in case of proper calibration of the strut parameters [5], [6].

Other recent studies also highlight that strut width formulation and material parameter selection have great potential effect on capacity curve and displacement demand estimation [11]. These results suggest

P-ISSN : 2598-1277
E-ISSN : 2621-3966

that an evaluation framework for standard RC infill residential houses should take infill effects into account to prevent false conclusions.

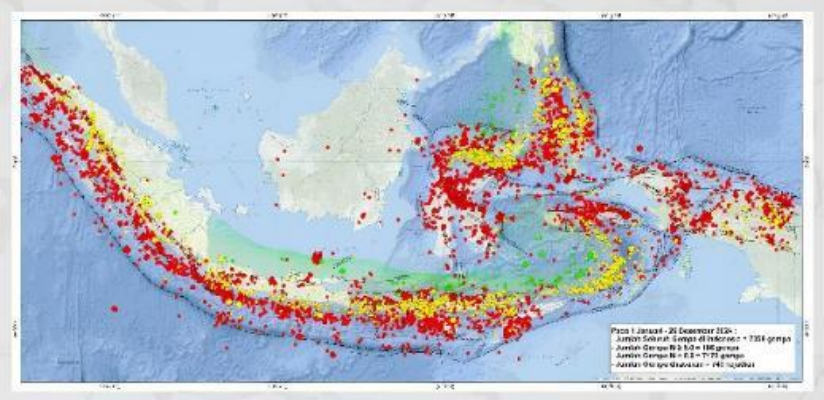

Figure 1. Seismicity Map of Indonesia 2024 [1]

Nonlinear static pushover analysis is frequently employed for performance based evaluation of existing buildings to determine global capacity curves, identify plastic hinge development, and estimate damage levels at a target displacement demand. FEMA 356 gives guidance on acceptance criteria for hinge performance states namely Immediate Occupancy (IO), Life Safety (LS), and Collapse Prevention (CP) [7]. FEMA 440 also refines the model for the capacity spectrum process, allowing for a closer determination of displacement demand and performance point, leading to better stability characteristics and broader accuracy for nonlinear static assessment [8].

In this study, pushover analysis is selected rather than nonlinear time history analysis for three main reasons. First, the objective of this research is a comparative assessment across multiple standard house types and two loading directions, which requires a consistent and computationally efficient method to generate comparable capacity curves and performance points. Second, nonlinear time history analysis requires a set of ground motion records and appropriate scaling procedures, where record selection and scaling can introduce additional variability and uncertainty that may obscure structural differences between house types. Third, detailed dynamic modeling and calibration particularly for masonry infill behavior and damping characteristics can be demanding for typical housing stock with limited structural information. Therefore, pushover analysis with the FEMA 440 capacity spectrum approach is considered suitable for capturing the global nonlinear behavior and supporting practical evaluation for standard residential buildings.This paper evaluates the seismic behavior of four typical existing two-storey residential building types in West Bandung Regency under soft soil conditions. The buildings are classified into Types A–D based on floor area and are modeled as RC frames with masonry infill walls represented using equivalent diagonal struts. Nonlinear static pushover analyses are performed in SAP2000 along the X and Y directions, and performance points are determined using the FEMA 440 equivalent linearization procedure [9]. Despite the growing use of nonlinear capacity-based strategies in Indonesia for performance evaluation and loss related assessment [4], comprehensive studies focusing on multiple typical two-storey house configurations specifically in West Bandung Regency remain limited. This gap motivates the current study.

The objectives of this research are: (1) to obtain capacity curves and performance points for each building type in the X and Y directions, (2) to interpret hinge performance distribution at the performance point (IO/LS/CP) and identify whether dominant damage occurs in beams or columns, and (3) to compare the relative seismic performance among the four building types as a basis for practical evaluation of similar existing residential buildings in West Bandung Regency. The workflow aligns with common numerical structural assessment practices using SAP2000 and has also been reported in related JGST publications [12].

P-ISSN : 2598-1277
E-ISSN : 2621-3966

2. RESEARCH METHOD

2.1. Research Object and Scope

The study examines four ordinary two-storey RC residential house types (Type A–D) within West Bandung Regency. Building layout/area grouping to which the four building types according to structure and area, the four forms of Building are defined as: Type A (Building Area 94 m^2), Type B (Building Area 99 m^2), Type C (Building Area 133 m^2), Type D (Building Area 145 m^2). Different types of the units are evaluated under lateral loading in two primary directions (X and Y), and the extent that the plans and opening areas distribution and orientation of the lateral elements would produce potential directional susceptibility to loadings is considered.

2.2. Seismic Hazard and Design Spectrum

The seismic input for the present work is based on the Indonesian seismic design code [2], where the risk targeted Maximum Considered Earthquake (MCER) level (approximately 2% probability of exceedance in 50 years and widely understood as 2500 year return period) is used. The seismic parameters based on the location study occurs in West Bandung Regency [13].
The soft soil site condition is a case under consideration, and such response spectrum parameters as are suitable are established accordingly. In the following capacity spectrum approach the design spectrum is employed to determine performance point for each building type [14].

Table 1. Response Spectrum Design Parameters

Parameter	Value
Coordinates	(-6.866282114, 107.454966)
Site class	SE (soft soil)
PGA MCEG	0.5600 g
Ss	1.3489 g
S1	0.5600 g
Sds	0.77 g
Sd1	0.77 g
T0	0.20 s
Ts	1.00 s
TL	6.00 s

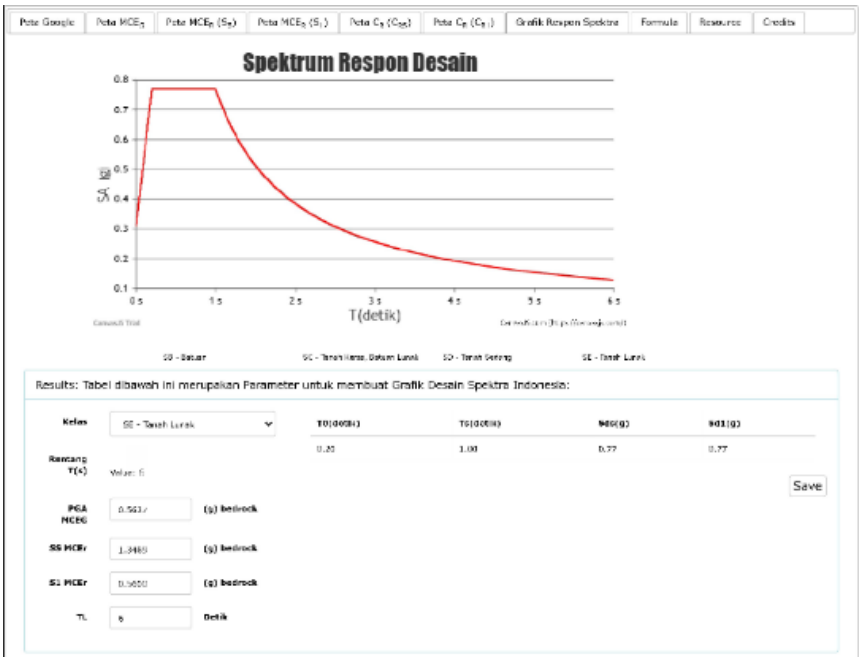

Figure 2. Elastic Response Spectrum Used in the Study [13]

P-ISSN : 2598-1277
E-ISSN : 2621-3966

2.3. Structural Modeling

Structural modeling was prepared using a workflow consisting of Revit (3D geometry) and SAP2000 (nonlinear analysis). The RC frame members (beams and columns) are modelled as frame elements following the structural dimensions and reinforcement arrangement. Floor slabs are modelled with a thickness of 120 mm and assigned as rigid diaphragms at each story to represent in plane stiffness and distribute lateral forces. Masonry infill walls are modelled using an equivalent diagonal strut approach (Section 2.4) with wall thickness taken as 200 mm including finishing [15].

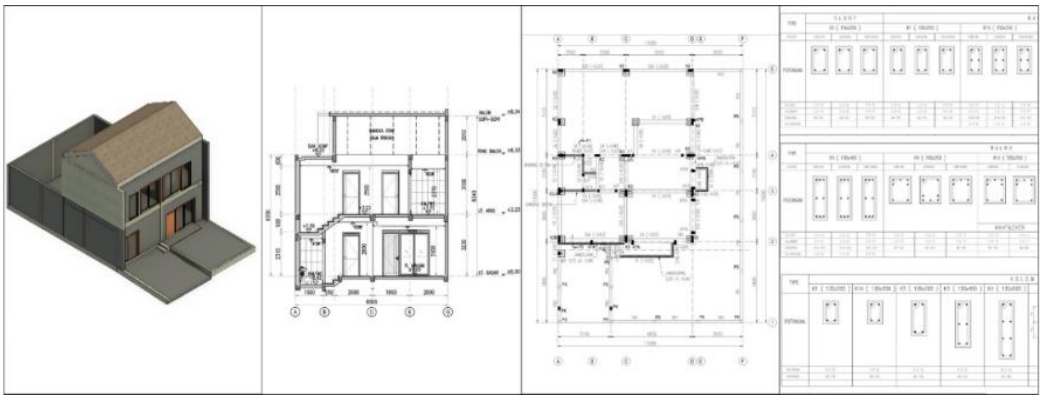

(a) (b) (c) (d)

Figure 3. Structural Data Type A: (a) 3D Revit model, (b) Building section, (c) Structural plan, (d) Structural details

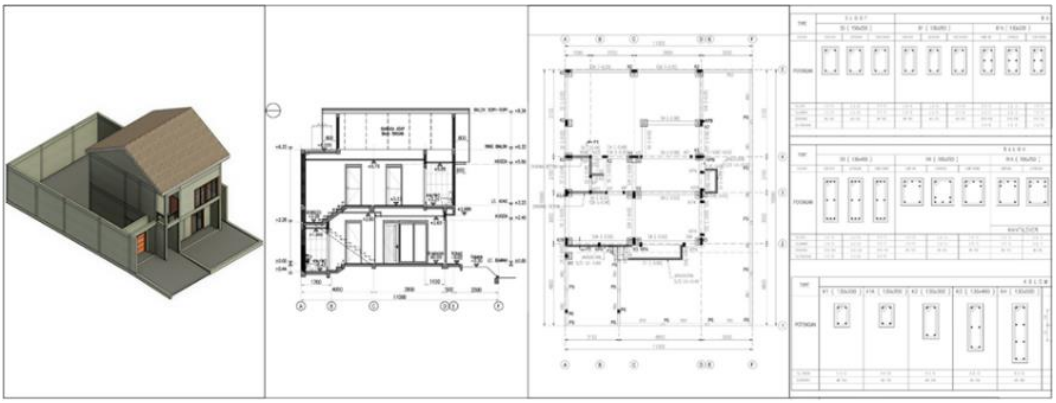

(a) (b) (c) (d)

Figure 4. Structural Data Type B: (a) 3D Revit model, (b) Building section, (c) Structural plan, (d) Structural details

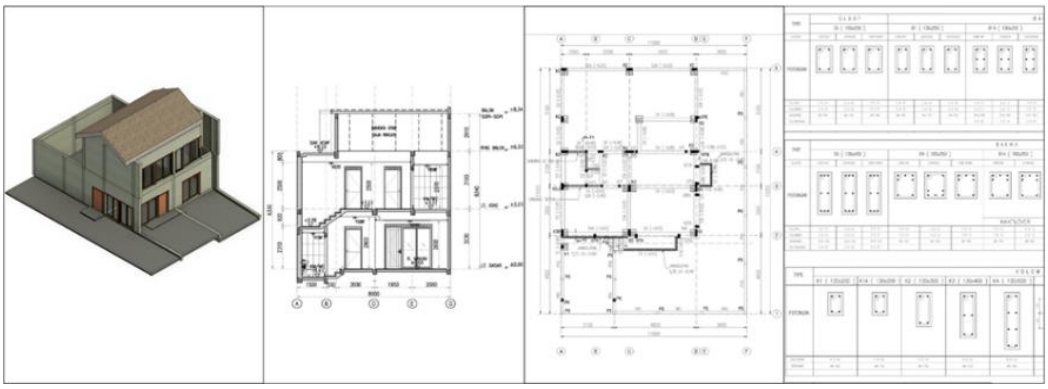

(a) (b) (c) (d)

Figure 5. Structural Data Type C: (a) 3D Revit model, (b) Building section, (c) Structural plan, (d) Structural details

P-ISSN : 2598-1277
E-ISSN : 2621-3966

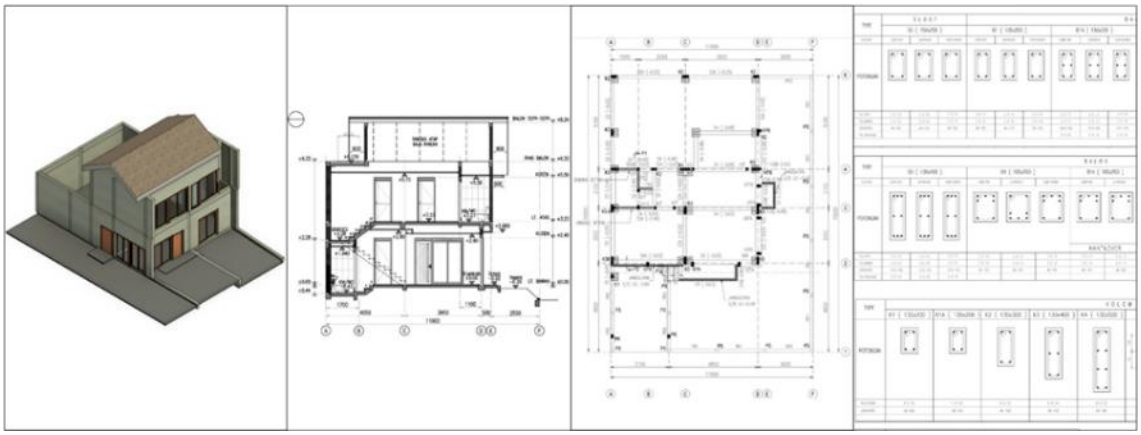

(a) (b) (c) (d)

Figure 6. Structural Data Type D: (a) 3D Revit model, (b) Building section, (c) Structural plan, (d) Structural details

Material properties are defined as concrete compressive strength $f'c = 18.68\ MPa$ and reinforcing steel yield strength $fy = 240\ MPa$ for longitudinal bars with $fy = 210\ MPa$ for stirrups. To represent stiffness degradation and cracking effects in nonlinear behaviour, stiffness modifiers are applied to key components: beams 0.35, columns 0.70, and slabs 0.25. Geometric nonlinearity is included by enabling P–Delta effects to account for additional second order moments under lateral drift and gravity loads. Accidental torsion of ±5% is included to reflect potential mass eccentricity and modelling uncertainties.

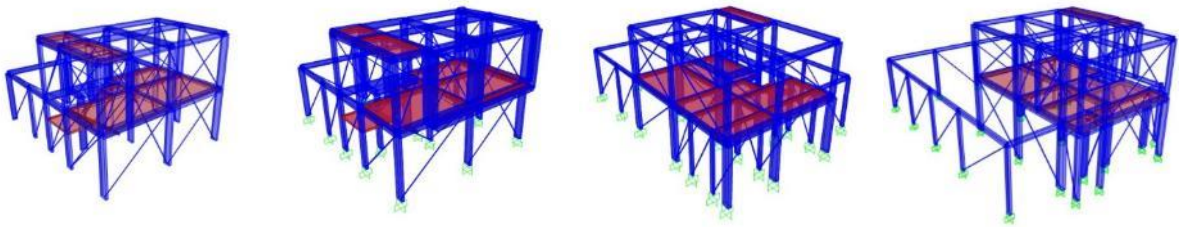

(a) (b) (c) (d)

Figure 7. SAP2000 Model and Strut Scheme: (a) Type A, (b) Type B, (c) Type C, (d) Type D

2.4. Equivalent Strut Model

Based on [16], the equivalent diagonal structure calculation is performed using Equations 1 to 2, where λ_1 is the coefficient for determining the equivalent width of the wall strut, E_m is the elastic modulus of the brick compressive strength, E_{fe} is the elastic modulus of the supporting frame material, t_{inf} is the thickness of the wall, h_{inf} is the height of the wall, I_{col} is the moment of inertia of the column, L_{inf} is the length of the wall, and a is the width of the equivalent strut structure width of the wall:

$$\lambda_1 = \left(\frac{E_m \times t_{inf} \times sin(2\theta)}{4 \times E_{fe} \times I_{col} \times h_{inf}}\right)^{0.25} \quad (1)$$

$$a = 0.175 \times (\lambda_1 \times h_{col})^{-0.4} \times L_{diag} \quad (2)$$

Brick walls with openings (doors/windows) are modeled as equivalent diagonal struts using the approach [17] with modifications to the effective area reduction in Equation (3):

$$A_{eff} = A\left(1 - \frac{Luas\ Bukaan}{Luas\ Total\ Dinding}\right) \quad (3)$$

P-ISSN : 2598-1277
E-ISSN : 2621-3966

Openings are classified into three categories: small (<10%) with a 10% reduction in axial stiffness, medium (10–20%) with a 25% reduction in stiffness, and large (>20%) with a 40% reduction in stiffness [5].

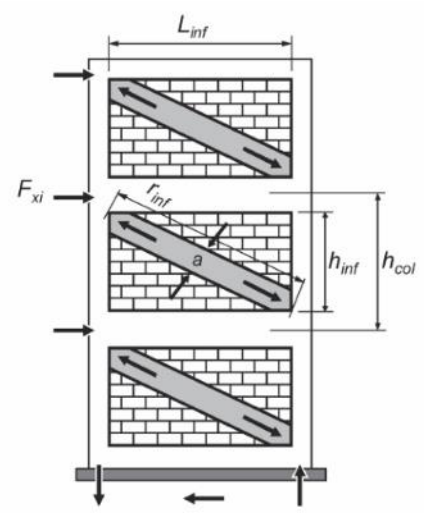

Figure 8. Strut Model [17]

2.5. Plastic Hinge Properties

Nonlinear behaviour is represented using concentrated plastic hinges assigned to beams and columns. Beam hinges are modelled as flexural (moment) hinges, while column hinges consider axial–flexural interaction to capture the influence of axial force on column nonlinear response. Hinge acceptance criteria are interpreted using [7] performance levels: Immediate Occupancy (IO), Life Safety (LS), and Collapse Prevention (CP). Hinge locations are placed at both ends of frame members to represent typical end region plasticity, enabling interpretation of mechanism tendency (beam dominant versus column dominant response) at the performance point.

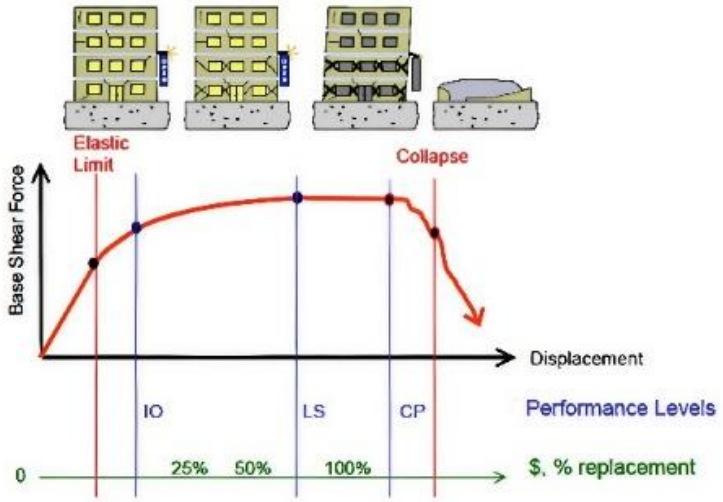

Figure 9. Plastic Hinge Performance Levels (IO, LS, CP) [14]

2.6. Pushover Procedure

Nonlinear static pushover analyses are performed in two directions: X direction (PAX) and Y direction (PAY). Lateral load distributions are defined based on dominant modal participation for each direction to represent realistic deformation patterns in the global response. A displacement controlled pushover is applied by monitoring roof displacement at the centre of mass; the target monitored displacement is set at 150 mm (approximately 2–5% of total building height). For the X direction pushover, the control

P-ISSN : 2598-1277
E-ISSN : 2621-3966

DOF is U1; for the Y direction pushover, the control DOF is U2. P–Delta effects remain enabled during pushover to capture second order demand consistently.

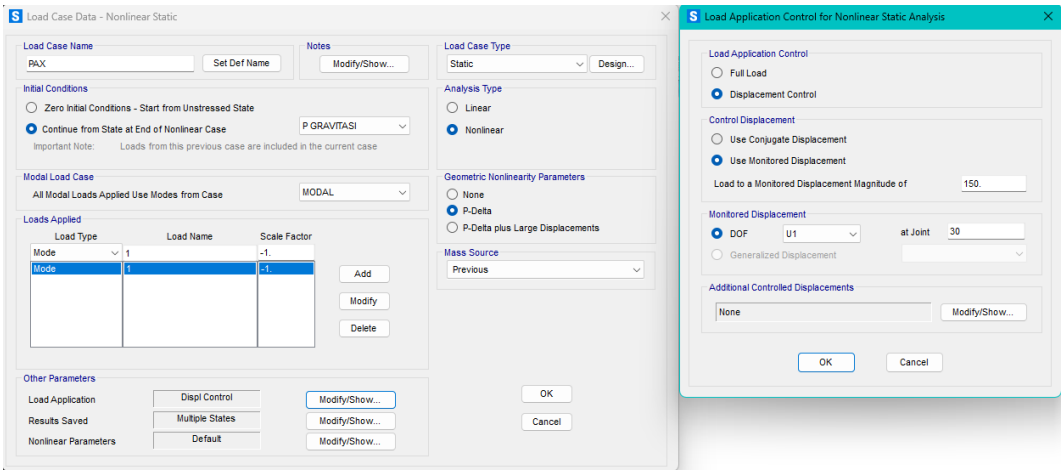

Figure 10. PAX Load Case Input

The pushover output (base shear versus roof displacement) is converted into ADRS format (spectral acceleration S_a versus spectral displacement S_d to apply the capacity spectrum method. The performance point is determined using the FEMA 440 Equivalent Linearization procedure by locating the intersection of the capacity spectrum and demand spectrum while iteratively updating effective damping and effective stiffness to account for nonlinear response.

3. RESULT AND DISCUSSION

3.1. Pushover Capacity Curve and Performance Point

Across the eight cases, the spectral acceleration at performance point (Sa) shows a relatively narrow band (approximately 1.09–1.34 g), indicating that the overall lateral strength level among the configurations is comparable. In contrast, the spectral displacement (Sd) and ductility demand (μ) vary more significantly (Sd about 11.9–48.0 mm; μ about 1.0-3.17). This pattern implies that the performance differences between types and directions are governed primarily by stiffness and deformation capacity (reflected in Sd and μ), rather than by strength alone (Sa).

Table 2. Structural properties and modeling inputs

Type	Plan area	Stories	Story height	Total height	Slab thickness	Beam sections (cm)	Column sections (cm)	$f'c$	fy	Cracked modifiers (SAP2000)	Infill thickness
A	94 m²	2	3.30 m, 3.03 m	6.33 m	120 mm	25/13, 25/15, 25/20, 30/13, 30/15, 30/20, 30/25, 30/30, 40/13	30/13, 40/13, 50/13	18.68 MPa	240 MPa (main); 210 MPa (ties)	beams 0.35Ig; columns 0.70Ig; slabs 0.25Ig	200 mm
B	99 m²	2	3.30 m, 3.03 m	6.33 m	120 mm	25/13, 25/15, 25/20, 30/13, 30/15, 30/20, 30/25, 30/30, 40/13	30/13, 40/13, 50/13	18.68 MPa	240 MPa (main); 210 MPa (ties)	beams 0.35Ig; columns 0.70Ig; slabs 0.25Ig	200 mm
C	133 m²	2	3.675 m, 3.350 m	7.025 m	120 mm	20/13, 25/13, 30/13, 40/15, 47/15, 50/17	25/13, 35/15, 50/20	18.68 MPa	240 MPa (main); 210 MPa (ties)	beams 0.35Ig; columns 0.70Ig; slabs 0.25Ig	200 mm
D	145 m²	2	3.675 m, 3.350 m	7.025 m	120 mm	20/13, 25/13, 30/13, 40/15, 47/15, 50/17	25/13, 35/15, 50/20	18.68 MPa	240 MPa (main); 210 MPa (ties)	beams 0.35Ig; columns 0.70Ig; slabs 0.25Ig	200 mm

P-ISSN : 2598-1277
E-ISSN : 2621-3966

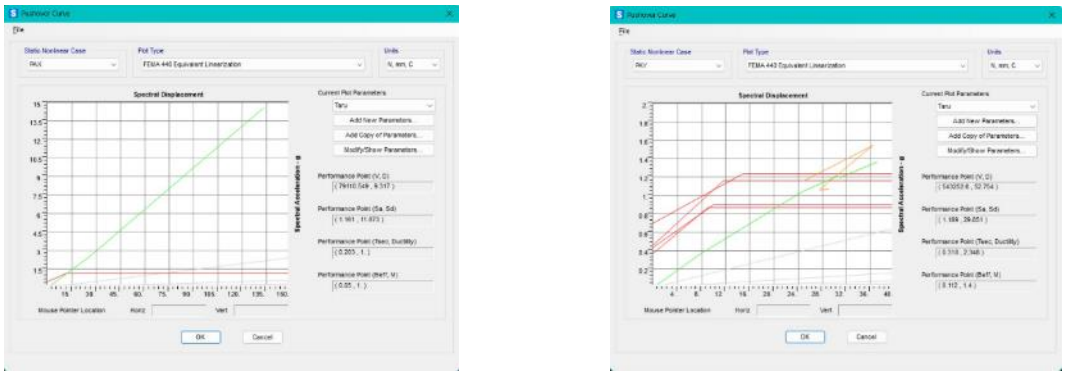

(a) (b)

Figure 11. Pushover curves and performance point of Type A: (a) X direction, (b) Y direction

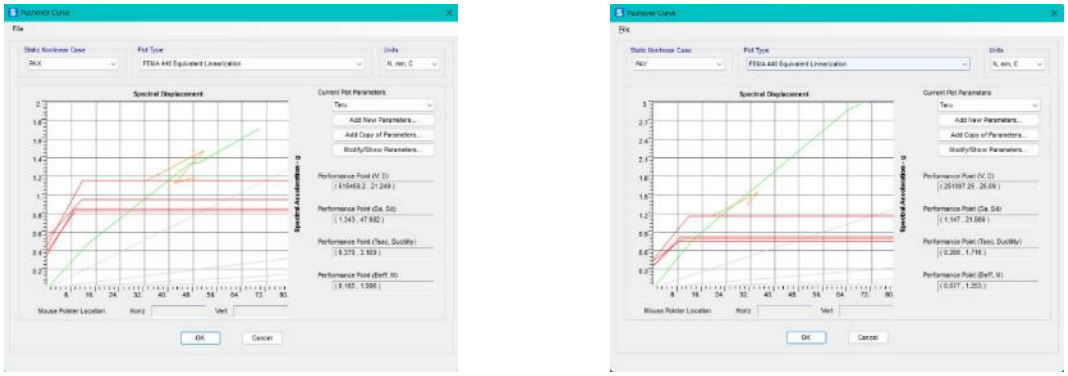

(a) (b)

Figure 12. Pushover curves and performance point of Type B: (a) X direction, (b) Y direction

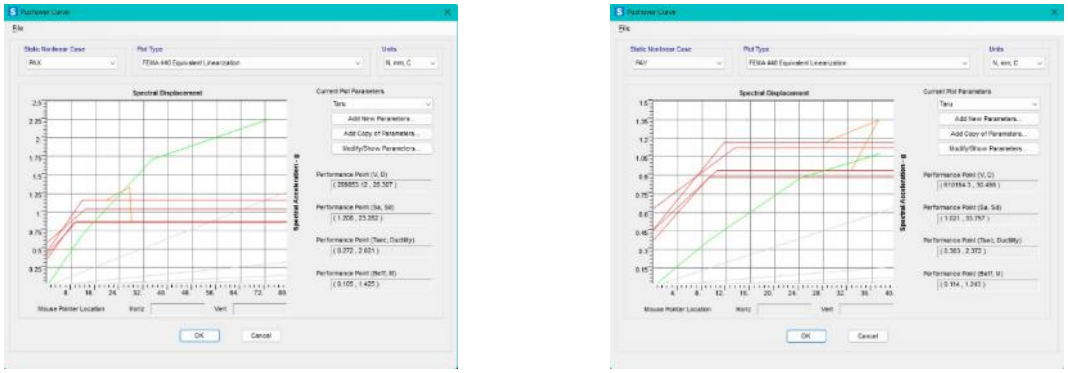

(a) (b)

Figure 13. Pushover curves and performance point of Type C: (a) X direction, (b) Y direction

(a) (b)

Figure 14. Pushover curves and performance point of Type D: (a) X direction, (b) Y direction

P-ISSN : 2598-1277
E-ISSN : 2621-3966

Table 3. Summary of FEMA 440 performance point parameters

Model	Direction	Sa (g)	Sd (mm)	μ	Roof disp (mm)	Base shear (kN)	Beff	Tsec (s)
Type A	X (PAX)	1.161	11.873	1.000	9.317	79.111	0.050	0.203
Type A	Y (PAY)	1.189	29.851	2.348	52.754	543.253	0.112	0.318
Type B	X (PAX)	1.343	47.982	3.169	21.249	515.459	0.165	0.379
Type B	Y (PAY)	1.147	21.989	1.716	25.090	251.097	0.077	0.266
Type C	X (PAX)	1.318	24.677	2.413	29.355	309.681	0.126	0.269
Type C	Y (PAY)	1.085	40.741	3.081	39.361	683.302	0.163	0.380
Type D	X (PAX)	1.138	35.199	2.219	50.219	481.864	0.116	0.339
Type D	Y (PAY)	1.153	17.260	1.457	24.852	387.118	0.073	0.239

Directional dependence is evident and differs by building type. Type A exhibits the strongest anisotropy: in PAX the response is essentially elastic ($\mu \approx 1$), while in PAY the system becomes moderately inelastic ($\mu > 2$) with substantially higher deformation demand. Type B shows the opposite tendency, where PAX produces the largest Sd and μ among all cases, indicating that this direction is the most flexible and demands the highest inelastic deformation. Type C demonstrates a higher inelastic demand in PAY than in PAX, while Type D shows moderate inelasticity in PAX and a comparatively lower deformation/ductility demand in PAY. These contrasts confirm that plan configuration, stiffness distribution, and infill/structural layout lead to direction specific performance that cannot be represented reliably using only one axis

From a seismic performance standpoint, cases with larger Sd and μ are expected to experience more pronounced nonlinear action and higher damage potential at the same hazard level, even if Sa is similar. Therefore, the loss risk evaluation should emphasize deformation related indicators (Sd, μ), not strength indicators alone.

3.2. Plastic Hinge Performance and Damage Level at Performance Point

Plastic hinge performance was evaluated according to FEMA 356 criteria (IO, LS, CP) at the step corresponding to the performance point [7]. The hinge development pattern indicates whether the structure tends toward a favorable beam sway mechanism (*strong column–weak beam*) or an unfavorable column sway mechanism.

Based on the verified dominant hinge locations at the performance point:

1. Type A : beam-dominant (PAX and PAY)
2. Type B : beam-dominant (PAX and PAY)
3. Type C : beam-dominant (PAX and PAY)
4. Type D : beam-dominant (PAX and PAY)

This implies that all house types show a more desirable mechanism (beam hinging). The hinge state distribution at the performance point extracted from SAP2000 output is summarized in Table 4.

Table 4. Hinge state distribution at the performance point

Model	Direction	Total Hinges	A–B	B–IO	IO–LS	LS–CP	CP–C	C-D	Notes
Type A	X (PAX)	190	189	1	0	0	0	0	Near elastic behavior
Type A	Y (PAY)	190	137	32	14	3	4	0	Significant damage
Type B	X (PAX)	242	185	47	9	0	0	1	Local failure detected
Type B	Y (PAY)	242	176	43	12	2	5	0	Significant damage
Type C	X (PAX)	198	169	29	0	0	0	0	Mostly B→IO
Type C	Y (PAY)	198	127	71	0	0	0	0	Mostly B→IO
Type D	X (PAX)	250	194	52	0	0	4	0	Extensive yielding
Type D	Y (PAY)	250	165	83	0	0	2	0	Extensive yielding

The hinge state distribution at the performance point is summarized in Table 4. Across all building types and loading directions, most hinges remain concentrated within the early to moderate damage ranges, particularly A–B, B–IO, and IO–LS, indicating relatively stable nonlinear behavior at the evaluated

P-ISSN : 2598-1277
E-ISSN : 2621-3966

demand level. Nevertheless, several cases exhibit localized progression into more advanced states (LS–CP and CP–C), and an isolated occurrence of C–D is observed, which should be treated as a critical warning sign even if it does not represent the dominant response. These results suggest that the overall structural response remains primarily controlled by beam plasticity; however, localized severe hinge formation may govern damage concentration and should be addressed through member level detailing and strengthening at the identified critical locations.

3.3. Comparison Between Building Types and Directional Response

A comparison of the four types of buildings shows that seismic response depends on loading direction considerably as indicated by differences in Sa, Sd, roof displacement at the control node, and demand for ductile capacity (μ) toward performance point. In general, the X direction responses are more prevalent for displacement and ductility among building types, indicating that there is more variation for lateral stiffness and yielding characteristics in this direction. In contrast, a number of Y direction cases achieve comparatively greater displacement demands at comparable or higher spectral intensities, indicating directional irregularity and the existence of stiffness imbalance effects.

Type A has the most minimal displacement and almost elastic behaviour ($\mu \approx 1$) in the X direction signifying little nonlinear demand at the performance point. Types B, C, and D show progressively larger Sd and roof displacement, accompanied by higher μ values, reflecting more pronounced inelastic deformation capacity and demand. In X direction cases, Type D also exhibits the highest degree of inelastic demand ($\mu \approx 3.8$) and the biggest proportion of roof displacement.

In the Y direction, there is even greater dichotomy in terms of building types. Several models have a moderate level of ductility ($\mu = 1.7 - 2.4$), however Type D shows significantly increased ductility requirement and highest Sd/Roof displacements at the performance point. This suggests that Type D's Y direction response is determined by very high post yield deflection (due to relatively low active stiffness, a higher deformation concentration, or both together). This directional sensitivity in practice means that there should be no single principal direction of seismism evaluation and retrofit prioritization, rather both directions should be evaluated to establish the controlling demand scenario of each building type.

The displacement based results are translated into global drift demand which relates to the roof displacement at the control node and this can be transformed into a drift ratio relationship (roof displacement divided by total building height). This linkage offers a direct line to talk about performance objectives (e.g., immediate occupancy versus life safety) in and beyond pre-established deformation limits and facilitates transparent reporting of results in terms of damage potential.

3.4. Implications for Seismic Performance Evaluation

The tested models demonstrate a largely beam dominant nonlinear mechanism at the performance level, which is in line with a ductile seismic response approach, in which plasticity is preferentially formed in the beams rather than columns. Such behavior is advantageous due to preventing story mechanisms induced by column degradation and promoting a more solidified redistribution of internal forces for inelastic response. Hence considering the global mechanism, it is apparent that the buildings exhibit favorable building strength/deformation hierarchy.

However, the hinge state distributions suggest that, still, in some circumstances and directions, localized extreme hinge states are possible. So perhaps, in general beam dominant mode performance can still be affected by defects of some members (e.g., detailing defects, local stiffness break, or deformation concentration close to critical beam column joints). Thus, efforts to improve protection methods should concentrate on preventing the localized damage, improving confinement and capacity to resist loading, joint performance at critical points, preventing potential loss point migration of stresses in the column and loss of gravity load carrying stability under the loading load.

Lastly, the transformation of roof displacement at performance point into drift demand is useful to allow performance level discussion and make the compare with the acceptance criteria of deformation. It also provides the data needed for retrofit prioritization as it guides the governing direction and type of building to the extent that drift-relevant demand is the most important over the base shear or spectral acceleration metrics of the existing building.

P-ISSN : 2598-1277
E-ISSN : 2621-3966

4. CONCLUSION

By using the FEMA 440 Equivalent Linearization process, performance points in two orthogonal directions (PAX and PAY) were identified, while key performance measures (Sa, Sd, Tsec, μ, and Beff) were extracted for comparison.

Key performance measures (Sa, Sd, Tsec, μ) were statistically analyzed during the process of simulation to predict the seismic characteristics. The findings suggest that, on the performance point, Sa's are mostly similar between the studied cases and Sd and ductility demand (μ) clarify the determination of seismic performance. The maximum deformation and inelastic pressures are observed for Type B PAX (Sd = 47.982 mm; μ = 3.169) and Type C PAY (Sd = 40.741 mm; μ = 3.081), indicating that these configurations/directions are most sensitive to deformation induced damage under the same seismic load. In contrast, Type A PAX presents near elastic behavior (Sd = 11.873 mm; μ = 1.0), that indicates the stiffest response of the cases. The FEMA 440 roof displacement output at the performance point can be associated with interstory drift to address performance effects where an interstory drift is a key component in damage and performance level in performance based assessment. When the structure is of two stories, the roof displacement demand is typically equal to the drift demand given total height and or story height. On the performance track scenario the more massive roof displacement you use, the more drift demand would correspond to the more likely to crack propagation/friction and damage accumulation from this point on in real-world instances. Thus, the directional differences observed (PAX vs PAY) make it clear that a building can show acceptable performance in one direction but high drift and inelastic demand in the orthogonal direction.

Mechanism-wise, this updated pushover runs demonstrate that hinge development is mostly beam dominant, which is generally preferred to column dominant mechanisms since it satisfies strong column weak beam principles. On the contrary, drift sensitivity damage may increase in configurations that have more demand for roof displacement than at the proposed level, where seismic demand becomes too high. Accordingly, the fundamental practical implication is the need to consider layout and stiffness distribution (infill wall contribution, placement of lateral resistors, etc.) explicitly in existing residential building evaluation, and two direction pushover assessment is necessary to capture the best demand direction.

In future study, the performance based evaluation may be improved by (i) directly presenting the drift ratios based on both roof displacement and story heights, and (ii) expanding the model to other representative house plans and soil/site variation to increase the transferability of the analysis for the regional housing stock.

REFERENCES

[1] Pusat Studi Gempa Nasional, *Bahaya Gempa Indonesia Untuk Perencanaan dan Evaluasi Infrastruktur Tahan Gempa*. 2024.

[2] Badan Standardisasi Nasional, “SNI 1726:2019 Tata cara perencanaan ketahanan gempa untuk struktur bangunan gedung dan nongedung,” *Tata cara perencanaan ketahanan gempa untuk struktur bangunan gedung dan nongedung*, pp. 1–248, 2019.

[3] K. K. Kuria and O. K. Kegyes-Brassai, “Pushover Analysis in Seismic Engineering: A Detailed Chronology and Review of Techniques for Structural Assessment,” *Applied Sciences (Switzerland)*, vol. 14, no. 1, 2024, doi: 10.3390/app14010151.

[4] J. R. Sugianto, C. Lesmana, and R. Milyardi, “Comparative Analysis of Earthquake Loss Estimation Using HAZUS Method with Modified Building Capacity Curve,” *Reka Buana : Jurnal Ilmiah Teknik Sipil dan Teknik Kimia*, vol. 9, no. 2, pp. 192–208, 2025, doi: 10.33366/rekabuana.v9i2.5676.

[5] L. D. Decanini, L. Liberatore, and F. Mollaioli, “Strength and stiffness reduction factors for infilled frames with openings,” *Earthquake Engineering and Engineering Vibration*, vol. 13, no. 3, pp. 437–454, 2014, doi: 10.1007/s11803-014-0254-9.

P-ISSN : 2598-1277
E-ISSN : 2621-3966

[6] P. Asteris, S. Antoniou, D. Sophianopoulos, and C. Chrysostomou, "Mathematical Macromodeling of Infilled Frames: State of the Art," *Journal of Structural Engineering*, vol. 137, pp. 1508–1517, Dec. 2011, doi: 10.1061/(ASCE)ST.1943-541X.0000384.

[7] FEMA 356, "Prestandard and commentary for the seismic rehabilitation of buildings," no. November, 2000.

[8] FEMA 440, "Improvement of Nonlinear Static Seismic Analysis Procedures," *Federal Emergency Management Agency*, no. June, p. 392, 2005.

[9] B. A. Reference, "Computers and Structures, Inc. Berkeley, California, USA," no. November, pp. 1–96, 1998.

[10] P. Usta, Ö. Onat, and Ö. Bozdağ, "Effect of masonry infill walls on the nonlinear response of reinforced concrete structure: October 30, 2020 İzmir earthquake case," *Eng. Fail. Anal.*, vol. 146, p. 107081, Apr. 2023, doi: 10.1016/J.ENGFAILANAL.2023.107081.

[11] A. Messaoudi, R. Chebili, H. Mohamed, A. Furtado, and H. Rodrigues, "The In-Plane Seismic Response of Infilled Reinforced Concrete Frames Using a Strut Modelling Approach: Validation and Applications," *Buildings*, vol. 14, no. 7, 2024, doi: 10.3390/buildings14071902.

[12] N. Gumelar, "Journal of Green Science and Technology Analysis and Design Structure of," *Journal of Green Science and Technology*, vol. II, no. 1, pp. 23–28, 2020.

[13] PUSGEN, "Peta Percepatan Puncak Dan Spektrum Respons," Jakarta, 2017.

[14] ATC 40, "ATC 40 Seismic Evaluation and Retrofit of Concrete Buildings Redwood City California," *Seismic safety commisionsion*, vol. 1, no. November 1996, p. 334, 1996.

[15] S. 2847, "PENETAPAN STANDAR NASIONAL INDONESIA 2847 : 2019 PERSYARATAN BETON STRUKTURAL UNTUK BANGUNAN GEDUNG DAN PENJELASAN SEBAGAI REVISI DARI STANDAR NASIONAL INDONESIA 2847 : 2013," no. 8, 2019.

[16] FEMA 273, "NEHRP Guidelines and Commentary for the Seismic Rehabilitation of Buildings," 1997. doi: 10.1193/1.1586092.

[17] R. J. Mainstone, "On the stiffnesses and strengths of infilled frames, Proc., Instn. Civ. Engrs., Supp. (iv), 57-90.," 1971.